Available online at www.sciencedirect.com

ScienceDirect

Energy Procedia 105 (2017) 4053 – 4058

Energy Procedia

The 8th International Conference on Applied Energy – ICAE2016

Numerical Modelling of a Dual Electrolyte Membraneless Electrolytic Cell for CO_2 to Fuel Conversion

Xu Lu[a], Dennis Y.C. Leung[a,*], Huizhi Wang[b], Jin Xuan[b]

[a]*Department of Mechanical Engineering, The University of Hong Kong, Pokfulam Road, Hong Kong*
[b]*Institute of Mechanical, Process and Energy Engineering, School of Engineering and Physical Sciences, Heriot-Watt University, Edinburgh, EH14 4AS, UK*

Abstract

This paper reports a mathematical model for the calculation of various losses in a dual electrolyte membraneless electrolytic cell (DEME) for CO_2 to formic acid conversion. The microfluidic characteristics of the cell were explored. Based on the electrochemical equilibrium states, major limiting factors, including mass transfer constraints, kinetic losses, and overpotentials, were considered. In particular, the acid-base interface and the neutralization losses therein were identified. We also quantified the electrical resistance losses on electrodes and within the micro-channels. Computational results were validated against previous experimental data. To our best knowledge, this is the first model studying the dual electrolyte arrangement and the associated losses, which can be used to develop future parametric optimization strategies.

Peer-review under responsibility of the scientific committee of the 8th International Conference on Applied Energy.

Keywords: CO_2 utilization; Dual electrolyte; Membraneless; Modelling; Electrochemistry.

Nomenclature

L'	hydraulic diameter	μ	fluid viscosity	ν	characteristic velocity for Reynolds number calculation
ρ	electrolyte density	Re	Reynolds number	E^0	equilibrium potential
R	universal gas constant	T	temperature	F	*Faraday constant*
K	equilibrium constant	α	charge transfer coefficient	j^0	partial current density at 0 V
η	electrode overpotential	c	local reactant concentration	z	electron transfer number of the rate determining step
D_{H^+}	Diffusion coefficient of H^+	D_{OH^-}	Diffusion coefficient of OH^-	p	pressure

* Corresponding author. Tel.: +852 2859 7911; fax: +852 2858 5415.
E-mail address: ycleung@hku.hk.

Peer-review under responsibility of the scientific committee of the 8th International Conference on Applied Energy.
doi:10.1016/j.egypro.2017.03.856

Pe	Peclet number	X	concentration of H^+	Y	concentration of OH^+
u	velocity	R′	resistance	$L_{interface}''$	length of the acid-base interface
$L_{catholyte}''$	length of catholyte	$L_{anolyte}''$	length of anolyte	S	surface area
σ	conductivity	ρ′	resistivity	t	thickness of the acid-base interface
I	current density	ϕ	level set function	Q_d	flow rate of gas
Q_c	flow rate of liquid	λ	Interfacial tension between gas and liquid	μ_c	viscosity of liquid
T-junction geometry	dimensionless parameter of the micro-channel	F_{st}	surface tension force	γ	stabilization parameters

1. Introduction

Electrochemical conversion of CO_2 to fuel can contribute to both carbon mitigation and renewable energy storage because of the highly controllable process under mild operation conditions; however, the performance of current available systems should be further improved in terms of reactivity and selectivity. With the innovative dual electrolyte technique[1], we have applied an acidic catholyte and an alkaline anolyte to decrease the overpotentials of the cell, enhancing the current density and reactivity. A state-of-the-art membraneless network was introduced and incorporated, with which not only would the cost be significantly reduced, some existing limitations could also be addressed, such as minimizing water management, alleviating salting-out issue and lowering ohmic loss. Thermodynamically favored pHs were identified to be 2 for catholyte and 14 for anolyte, achieving a tripled reactivity compared with a conventional single electrolyte arrangement and an improved peak Faradaic efficiency of 95.6%[1]. Experiment-based parametric study was conducted in the followed-up work[2], identifying the possible improvement by optimizing the catalyte to Nafion ratio, feedstock flow rates, and micro-channel dimensions.

However, present experimental efforts are not sufficient to obtain a comprehensive and deep understanding of the intrinsic mechanisms, particularly with regard to the micro-level species transport and the acid-base interface. Therefore, a mathematical model is established in this work to investigate the electrochemical fundamentals involved and the polarization characteristics. Mass transfer constraints, kinetic losses, overpotentials, neutralization energy dissipation, and electrical resistance losses are taken into account. Validated by related experimental results, this model could be a useful tool to develop optimization strategies for the reactor performance.

2. Methodology

2.1. Model description

This model considers a dual electrolyte membraneless electrolytic cell (DEME) as shown in Fig. 1 with dimensions listed in Table 1, which is equipped with parallel, rectangular, multi-layered channels and operates in a co-flow mode. CO_2 enters the cathode gas channel, while the anode is open to the atmosphere. Aqueous H_2SO_4 and KOH co-laminar electrolyte flows pass between two gas diffusion electrodes (GDEs). The cathode is coated with catalysts at the electrode-electrolyte interface. A silver current collector backs each GDE at the other side.

Table 1. Geometric parameters of the model

Parameter	Value	Parameter	Value	Parameter	Value	Parameter	Value	Parameter	Value
M	4 mm	N	7.5 mm	R	1.25 mm	m	3.75 mm	n	7 mm
r	1 mm	W	2 mm	L	5 mm	H	0.5 mm		

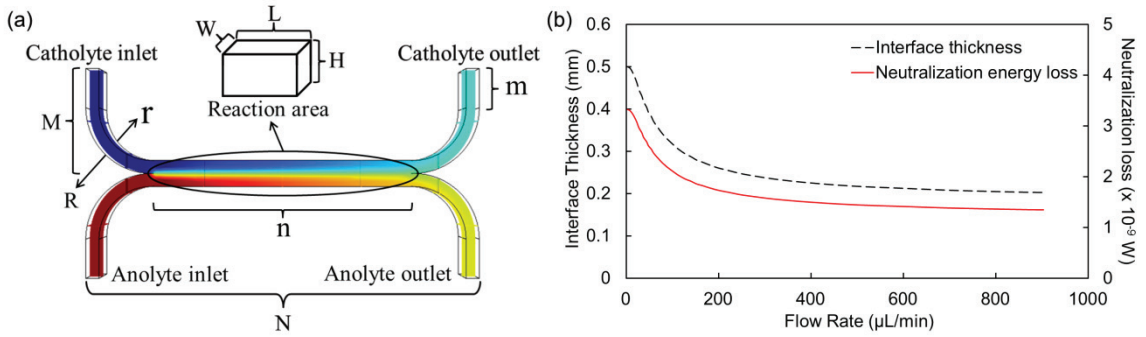

Fig. 1. (1) Schematic diagram of the DEME geometry and associated dimensional designation; and (b) Interface thicknesses and associated neutralization energy losses against flow rates

2.2. Mass transfer constraint

Four equilibrium states are assumed during the dissolution of gaseous CO_2 into the liquid electrolytes:

Absorption: $CO_2(g) \leftrightarrow CO_2(aq)$ ····· Equ. (1)

Hydrolysis: $CO_2(aq) + H_2O \leftrightarrow H_2CO_3$ ····· Equ. (2)

Overall: $CO_2(g) + H_2O \leftrightarrow H_2CO_3^*$, $[H_2CO_3^*] \equiv [CO_2(aq)] + [H_2CO_3]$ ····· Equ. (3)

Pseudo-equilibrium: $H_2CO_3^* \leftrightarrow H^+ + HCO_3^-$ ····· Equ. (4)

2.3. Kinetics

At 298K, the cathode reaction in acidic environment is:

$CO_2 + 2H^+ + 2e^- \rightarrow HCOOH$ ····· Equ. (5)

$2H^+ + 2e^- \rightarrow H_2$ ····· Equ. (6)

Anode reaction in alkaline environment is:

$2OH^- \rightarrow \frac{1}{2}O_2 + H_2O + 2e^-$ ····· Equ. (7)

The equilibrium potential of CO_2 reduction reaction comes from the Nernst equation, so do the cathode side reaction, hydrogen evolution reaction (HER), and the anode oxygen evolution reaction.

$$E_{cathode}{}^0 = E_{cathode\ @\ pH=0}{}^0 - \frac{RT}{2F} \cdot \ln\left(\frac{1+\frac{K_{ox1}}{[H^+]}\cdot\left(1+\frac{K_{ox2}}{[H^+]}\right)}{1+\frac{K_{red1}}{[H^+]}} \cdot \frac{1}{[H^+]^2}\right) \quad \text{Equ. (8)}$$

2.4. Overpotential

The overpotentials are related to the partial current densities and electrolyte pHs. Tafel law and the above-derived mass transfer constraint are applied:

$$\eta_{cathode} = E - E_{cathode}{}^0 = \frac{RT}{\alpha_{cathode} zF} \ln\left(\frac{j_{cathode}}{j_{cathode}{}^0} \cdot \frac{c_{CO_2}{}^0}{c_{CO_2}}\right) \quad \text{Equ. (9)}$$

$$\eta_{HER} = E - E_{HER}{}^0 = \frac{RT}{\alpha_{HER} zF} \ln\left(\frac{j_{HER}}{j_{HER}{}^0}\right) \quad \text{Equ. (10)}$$

$$\eta_{anode} = E - E_{anode}{}^0 = \frac{RT}{\alpha_{anode} zF} \ln\left(\frac{j_{anode}}{j_{anode}{}^0}\right) \quad \text{Equ. (11)}$$

2.5. Neutralization reaction loss

At catholyte pH=2 and anolyte pH=14, ion diffusion dominates the cross-electrolyte transfer mechanism because of the unbalanced acid-alkaline state[1]. In this case, the neutralization reaction area and its affiliated loss could be determined by a diffusion model[3] using a finite element analysis software, COMSOL Multiphysics (COMSOL Group).

2.5.1. Transport of concentrated species

In the present microchannel, the Re number is significantly less than 1, the steady state Navier-Stokes equations are applicable without the problematic convective term:

$$\nabla \cdot (\rho u) = 0 \quad \text{Equ. (12)}$$

$$\nabla p = -\rho u \cdot \nabla u + \mu \nabla^2 u + \rho g \quad \text{Equ. (13)}$$

2.5.2. Catholyte & anolyte interface

Fick's law can be used to describe the diffusive transport. The mass-balance equations for the solute are:

$$-\nabla \cdot (-D_{H^+} \nabla X + Xu) = 0 \quad \text{Equ. (14)}$$

$$-\nabla \cdot (-D_{OH^-} \nabla Y + Yu) = 0 \quad \text{Equ. (15)}$$

2.5.3. Diffusive flow characterization

Peclet number could be deduced to be $7132 \gg 1$, hence it is necessary to maintain numerical stability when solving the Fick's equation.

2.5.4. Boundary conditions

Constant species mass fraction and constant inlet velocity are prescribed at the inlets, while zero-diffusive flux of species and constant outlet pressure are for the outlets. On electrodes, non-flux boundaries are set. Non-slip condition is assumed for walls.

2.5.5. Neutralization reaction loss

The model outputs the concentration at the catholyte outlet, which could be used to derive the interface thickness. For 1 second, H^+ involved in neutralization reaction is $8.335 \times 10^{-11} \times t \, \mathrm{mol/s}$.

Under standard conditions, the neutralization reaction $H^+ + OH^- \rightarrow H_2O$ has a Gibb's free energy of $-79.9 \, \mathrm{kJ \, per \, mol \, H_2O \, formed}$.

Hence the neutralization energy loss rate could be expressed as $6.65 \times 10^{-6} \times t \, \mathrm{W}$.

2.6. Electrical resistance loss

The electrical resistance losses includes two sources: the carbon-supported electrodes and flowing electrolytes inside the micro-channel. Calculations are based on the definition:

$$R = \rho' \frac{L''}{S} = \frac{1}{\sigma} \times \frac{L''}{S} \quad \text{Equ. (16)}$$

3. Results and discussion

Table 2 shows he respective values used in this model. As indicated by its low Reynolds number ($\ll 1$), the electrolytes flow laminarly through the micro-channels. The catholyte and anolyte, with different pHs, are therefore separated by an effective mixing layer.

The bulk concentration of dissolved CO_2 (aq) is determined by the limitation of mass transfer under different electrolyte pHs. Assuming gas-liquid equilibrium of the reactant $CO_2(g)$, which is absorbed by the cathode from gas phase into the flowing catholyte and to the liquid/solid interface followed by hydrolysis, the bulk concentration of $CO_2(aq)$ could be obtained as $0.029 \, \mathrm{mol/L}$.

As for the kinetics, it reveals the impact of electrolyte pHs on equilibrium electrode potentials, which is unique for this model because of the co-existence of two different electrolyte pHs. The equilibrium potentials on cathode and anode sides were shown below:

$$E_{cathode}{}^0 = -0.042 - 0.012839 \cdot \ln\left(\frac{1+\frac{6.39}{X} \cdot \left(1+\frac{10.32}{X}\right)}{1+\frac{3.75}{X}} \cdot \frac{1}{X^2}\right) \quad \text{Equ. (17)}$$

$$E_{HER}{}^0 = -0.059pH - 7 \times 10^{-8} \quad \text{Equ. (18)}$$

$$E_{anode}{}^0 = -0.059pH + 1.2291 \quad \text{Equ. (19)}$$

Another two major losses are overpotentials on electrodes and neutralization losses within the acid-base interface. The former could be prescribed by the Tafel law and the latter is plotted in Fig. 1 (b). Numerical model indicates that at a flow rate of 500 μL/min, the output concentration of KOH is 0.22 mol/m^3, hence $t_{500} = 0.22$ mm. In this case, the neutralization energy loss rate equals to 1.463×10^{-9} W, contributing an insignificant voltage loss to the whole cell polarization.

In terms of electrode electrical resistance, given that $\rho' L'' = 5.5\ m\Omega \cdot cm^2$ (Shanghai Hesen Electrical) and the surface area $S = 0.1\ cm^2$, it is calculated to be 0.055Ω.

For electrolyte resistance, three zones should be considered: catholyte, interface and anolyte, whose effective lengths are derived at the end side of the interface. It should be noted that the resistance of catholyte at room temperature should be based on the resistivity of K_2SO_4 solution for the sake of a workable conductivity[4]. The molar conductivity of 0.5 mol/L aqueous K_2SO_4 solution is referenced at $\sigma = 0.078\ S/cm$[5]. Accordingly, the resisivity of the catholyte is 2.82 Ω. The resistance of the anolyte at room temperature could be simply determined by the resistance chart[6], stating that the conductivity of 1 mol/L KOH solution at 25℃ is 0.2153 S/cm. Thus the resistivity of the anolyte is 1.02 Ω.

On the other hand, the electrolyte within the interface zone could be regarded as a mixture of 1.98 mol/L KOH and 0.5 mol/L K_2SO_4 considering the offset due to acid-base neutralization reaction. The theory of Debye and Hückel[7] implies that the sum of conductivity contributed from two electrolyte solutions are additive, giving the conductivity of the electrolyte in the interface zone to be $0.2933\ S/cm$ and resistivity at 0.375 Ω.

Considering the above-mentioned equilibrium states and losses, Fig. 2 demonstrates a comparison between experimental results and mathematical model. Quantitatively, the difference between experimental and numerical approaches is less than 15% at the level of interest, validating the effectiveness of the mathematical model.

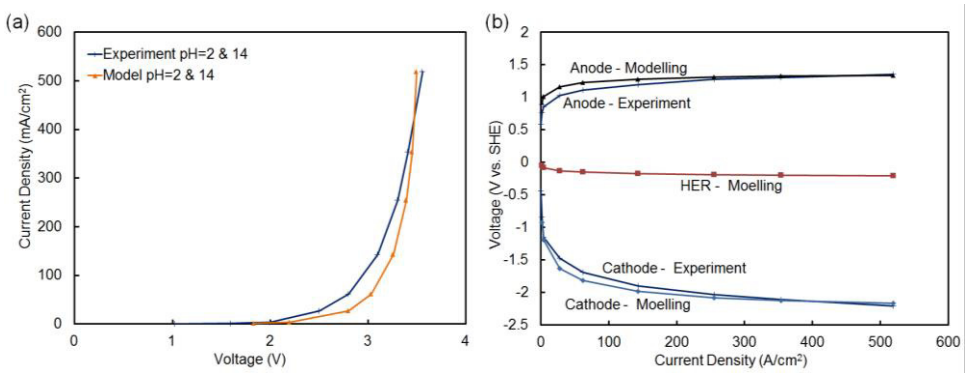

Fig. 2. (a) Polarization curves and (b) the corresponding individual electrode polarization curves of the DEME obtained by experiment and mathematical model.

Table 2. Values of key parameters of the model

Parameter	Value	Parameter	Value	Parameter	Value
L'	0.28 mm	μ	1 mPa · s	K'	$\frac{[H_2CO_3]}{[CO_2(aq)]} = 2.6 \times 10^{-3}$
$L_{interface}''$	0.11 mm	Re	0.0378	K_0	$\frac{[H_2CO_3^*]}{p_{CO_2}} = 2.94 \times 10^{-4}$
$L_{catholyte}''$	0.22 mm	λ	0.005 N/m	K_1	$(\gamma^2)\frac{[H^+][HCO_3^-]}{[H_2CO_3^*]} = 4.53 \times 10^{-7}$
$L_{anolyte}''$	0.22 mm	μ_c	0.002 Pa·s	R	$8.314\ JK^{-1}mol^{-1}$
$E_{cathode\ @\ pH=0}{}^0$	-0.042 V	γ	0.05 m/s	D_{H^+}	$9.31 \times 10^{-9} m^2 s^{-1}$
T-junction geometry	$\frac{\mu_c U_c}{\lambda}$	ρ	$1000\ kg/m^3$	D_{OH^-}	$5.30 \times 10^{-9} m^2 s^{-1}$
Pe	7132	T	$298K$	z	2

ν	0.135 m/s	F	96485 $Cmol^{-1}$	$\alpha_{cathode}$	-0.05
α_{HER}	-0.5	α_{anode}	0.16	K_{red1}	0.024
K_{ox1}	0.0017	K_{ox2}	0.000033	${j_{cathode}}^0$	0.01 $mAcm^{-2}$
${j_{HER}}^0$	0.0016 $mAcm^{-2}$	${j_{anode}}^0$	0.002 $mAcm^{-2}$		

4. Conclusion

This work has demonstrated an experiment-validated mathematical model for a DEME. The microfluidics and diffusive flow were characterized. Major losses were considered, such as mass transfer constraint, overpotentials and electrical resistance losses. Besides, this model presents the first systematic investigation on the acid-base co-existence system in a microfluidic reactor. It is found that the intrinsic kinetics could be notably altered by the dual electrolyte arrangement, whilst the neutralization energy dissipation is insignificant. Further numerical characterization of the electrolyte flow pattern and associated electrochemical performance in industrial-scale applications could be conducted. The effectiveness of this model also indicates its usefulness for future comprehensive parametric optimization to evaluate the effects of structural parameters, flow conditions and material properties.

Acknowledgements

This project is financially supported by the CRCG of the University of Hong Kong and the Scottish – Hong Kong SFC/RGC Joint Research Scheme XHKU710/14 and SFC Project H15009.

References

[1] Lu X, Leung DY, Wang H, Maroto-Valer MM, Xuan J. A pH-differential dual-electrolyte microfluidic electrochemical cells for CO2 utilization. Renewable Energy. 2016;95:277-85.

[2] Lu X, Leung DY, Wang H, Xuan J. A high performance dual electrolyte microfluidic reactor for the utilization of CO2. Applied Energy. 2016. (To appear)

[3] Finlayson BA, Aditya A, Brasher V, Dahl L, Dinh HQ, Field A, et al. Mixing of Liquids in Microfluidic Devices. COMSOL Conference, Boston2008.

[4] Vinal G, Craig D. Resistivity of sulphuric acid solutions and its relation to viscosity and temperature. J Res Natl Bur Stand US. 1934;13:689-97.

[5] Wolf AV. Aqueous solutions and body fluids; their concentrative properties and conversion tables. 1966.

[6] Gilliam R, Graydon J, Kirk D, Thorpe S. A review of specific conductivities of potassium hydroxide solutions for various concentrations and temperatures. International Journal of Hydrogen Energy. 2007;32:359-64.

[7] Wright MR. An introduction to aqueous electrolyte solutions: John Wiley & Sons; 2007.

Biography

Prof. Dennis Y.C. Leung received his B.Sc. (Eng.) and Ph.D. from the Department of Mechanical Engineering at the University of Hong Kong. He joined the same department in 1993 and is now a full professor of the department specializing in renewable energy and energy conservation. He is a specialty chief editor of the Frontiers in Environmental Sciences and editorial board member of several journals including Applied Energy.